Am J Cancer Res 2026;16(8):3660-3677
www.ajcr.us /ISSN:2156-6976/ajcr0173056

Original Article

Transcriptional regulation of ubiquitin specific peptidase 2b by farnesoid X receptor and its implications in the pathogenesis of hepatocellular carcinoma

Winifer Ali, Christina Nadolny, Xinmu Zhang, Qiwen Chen, Syed F Hashmi, Tasneem Huniti, Md Mosiqur Rahman, Lia Bozza, Danielle Warila, Ruitang Deng

Department of Biomedical and Pharmaceutical Sciences, College of Pharmacy, University of Rhode Island, 7 Greenhouse Road, Kingston, RI 02881, USA

Received April 2, 2026; Accepted June 10, 2026; Epub August 15, 2026; Published August 30, 2026

Abstract: Farnesoid X receptor (FXR) signaling plays an important role in liver regeneration and carcinogenesis. Dysregulation of FXR signaling is linked to the pathogenesis of hepatocellular carcinoma (HCC) while FXR knockout mice spontaneously develop HCC as they age. Ubiquitin specific peptidase 2b (USP2b) is a deubiquitinating enzyme regulating protein stability and other activities. In our recent study, we found that USP2b was significantly downregulated in subjects with HCC and exhibited both tumor-promoting and tumor suppressive activity in a context-dependent manner. However, the mechanistic link between FXR signaling and USP2b and its implications in the pathogenesis of HCC remain to be determined. In this study, we revealed that USP2b was transcriptionally regulated by FXR. Activation of FXR significantly increased while antagonizing FXR reduced USP2b mRNA and protein expression *in vitro* and *in vivo*. Consistently, USP2b expression was significantly reduced in FXR knockout (FXR-KO) mice. Further investigation showed that USP2b was transcriptionally regulated by FXR in an isoform-specific manner, predominantly by FXRα2 but not FXRα1. The transcription starting sites (TSS) of USP2 isoforms were determined by 5'RACE, which leads to the identification of the USP2b-specific promoter. An FXR response element (FXRE) was identified in the USP2b promoter and functionally characterized. FXR directly bound to the FXRE *in vitro* and recruited to the USP2b promoter in intact cells and *in vivo*. Further study revealed that upon FXR activation, co-activator-associated arginine methyltransferase 1 (CARM-1) was significantly recruited to the human USP2b promoter while coactivators glutamate receptor-interacting protein 1 (GRIP-1) and peroxisome proliferator-activated receptor-γ coactivator 1α (PGC-1α) were significantly recruited to the mouse USP2b promoter. Over-expression of USP2b in FXR-KO mice significantly slowed down tumor growth with reduced tumor size while maintained comparable tumor numbers consistent with its tumor suppressive activity. In summary, this study demonstrated that USP2b was transcriptionally regulated by FXR in an isoform-dependent manner and USP2b played a tumor-suppressive role in the pathogenesis of FXR deficiency-induced HCC.

Keywords: FXR, USP2, USP2a, USP2b, HCC, transcriptional regulation, ubiquitination and deubiquitination

Introduction

Hepatocellular carcinoma (HCC) is the sixth most common cancer and the third leading cause of cancer-related deaths in the United States [1]. Annual rates of liver cancer cases and death cases continue to increase over time [2]. HCC is usually diagnosed at later stages (III to IV) when patients have already developed a progressive disease [3]. Currently, the treatment options for HCC are limited and liver transplants are the only option if HCC is detected early.

The nuclear receptor farnesoid X receptor (FXR) has been well recognized as a master metabolic regulator and plays critical roles in maintaining the homeostasis of cholesterol, bile acids, glucose, and lipids [4, 5]. However, FXR also plays critical roles in liver regeneration and provides protection against HCC development. Dysregulation or decreased FXR expression is associated with the development of HCC [5-8]. In our previous study, we found that FXR isoform expression was markedly altered in HCC tumor tissues [9]. The FXR-α1/FXR-α2 ratios were significantly increased, with undetectable

https://doi.org/10.62347/UIYZ8333

FXR-α2 expression in one third of the HCC tumor samples. Consistently, FXR knockout (FXR-KO) mice spontaneously develop HCC tumors as they aged [6, 10]. However, the underlying mechanism by which FXR protects HCC development is not fully understood.

Ubiquitination is an enzymatic process that involves the binding of a ubiquitin to a substrate protein for subsequent proteasomal degradation of the ubiquitinated proteins [11, 12]. On the other hand, ubiquitin can be removed from ubiquitinated proteins by deubiquitinating enzymes [13, 14]. Therefore, protein stability is regulated by both ubiquitination and deubiquitination processes. Ubiquitin specific peptidase 2 (USP2) is a deubiquitinating enzyme known to play important roles in various physiological and pathological conditions [15-19]. Three USP2 isoforms have been reported including USP2a, USP2b and USP2c [20-22]. Among the 3 isoforms, USP2b is the predominant isoform expressed in the liver with USP2c below detection level [23]. In our previous study, we found that USP2b expression was significantly down-regulated in HCC subjects. USP2b exhibited tumor suppressive activities *in vitro* in HepG2 and Huh 7 cells by enhancing apoptosis [23]. However, the underlying mechanism by which USP2b was significantly down-regulated in HCC subjects and whether FXR regulates USP2b with implications in the pathogenesis of HCC remains to be determined.

In this study, we demonstrated that USP2b was transcriptionally regulated by the FXR signaling pathway in an FXR isoform-specific manner with FXRα2 being the predominant regulator. Activation of FXR significantly increased while antagonizing FXR reduced USP2b expression *in vitro* and *in vivo*. Dissection of the USP2b promoters led to identification of the functional FXR responsive element (FXRE) in the USP2b promoter. Upon activation, FXR and its coactivators were specifically recruited to the USP2b promoters. Further *in vivo* study with FXR-KO mice revealed that USP2b significantly slowed down HCC tumor growth with markedly reduced tumor size consistent with its tumor suppressive activity. The results thus demonstrated that FXR-mediated dysregulation of USP2b played a role in the pathogenesis of HCC.

Materials and methods

Chemicals and reagents

Obeticholic acid (OCA) (catalog #113945), GW-4064 (catalog #131851), and DY268 (catalog #1609564-75-1) were purchased from Chem Shuttle (Hayward, CA). Dimethyl sulfoxide (DMSO) (catalog #67-68-5) was purchased from Sigma (St. Louis, MO). The GenJet transfection reagents (catalog #SL100489) were purchased from Signagen Laboratories (Frederick, MD). Dual-luciferase promoter reporter assay system (catalog #E1980) was purchased from Promega (Madison, WI).

Plasmid constructs

Human FXRα2 and FXRα1 expression constructs were kindly provided by Dr. Matthew Stoner (University of Rhode Island, Kingston, RI) and Dr. David Mangelsdorf (University of Texas Southwestern Medical Center), respectively. Promoter reporter constructs were synthesized and purchased from Gene Universal (Delaware, USA). These promoter constructs were cloned with the promoter regions of USP2b (-1.5 kb) into the pGL3-basic vector containing the firefly luciferase gene. Element reporter constructs were also synthesized and purchased from Gene Universal. Element reporters consisting of three copies of the wild type (WT) or mutated USP2b-FXRE were constructed by cloning the elements into the pGL3-Promoter vector. The pRL-null vector with the wild type Renilla luciferase gene was used as the control reporter vector for luciferase activity normalization (catalog #E2271, Promega).

Cell culture

Human hepatoma cell line Huh 7 (catalog #HB-8065) were purchased from American Type Culture Collection (ATCC). Cells were cultured in DMEM (catalog #11965092, Thermo Fisher Scientific) supplemented with 1% penicillin-streptomycin (catalog #15140122, Thermo Fisher Scientific), 1% non-essential amino acids (catalog #13-114E, Lonza), and 10% fetal bovine serum (FBS) (catalog #LSAC12306C, Wilkem Scientific).

Short-term mouse studies

WT C57BL/6J mice (stock #000664) and FXR-KO mice (stock #007214) were obtained from the Jackson Laboratory (Bar Harbor, Maine).

Table 1. A list of oligonucleotides used in 5'RACE, EMSA and ChIP-PCR assays

Assays	Name of the oligos	Sequence of the Oligos
5'RACE	USP2a-5RACE-GSP1	ATTCTCGGGCTACACAACACACAG
	USP2a-5RACE-GSP2	TGATCAGCACACAGATGGCT
	USP2a-5RACE-GSP3	CTACATTTCTCACGTCCAGACTG
	USP2a-5RACE-GSP4	GCTGCCTTTGACACCCTACT
	USP2a-5RACE-GSP5	GAGTCTCAAAGCTGGTACTGAC
	USP2b-5RACE-GSP1	CAAGCCTGCGATCTCTAGGGATG
	USP2b-5RACE-GSP2	CCAGGAGACCCTTGGAAAAGAG
	USP2b-5RACE-GSP3	CGAGGAACATCTCGGGGATTC
	USP2b-5RACE-GSP4	CTCATGATAGACTGGGGTTGATC
EMSA	USP2b-FXRE wt	TGGAGAAAGGTCGCTGCAGTTTGTCCGGGGTCC
	USP2b-FXRE-Mut	TGGAGAAAAAAAAAAAAAAATTGTCCGGGGTCC
ChIP-PCR	hUSP2b-F	GATTCAGTCAGAGTCTGGGT
	hUSP2b-R	GTACACGCACACATGACCAC
	mUSP2b-F	GGGTGAAATGCTTGTGTGTG
	mUSP2b-R	ATTTTGAGCCTACGGGTGTG

Mice were fed a regular chow diet and treated with vehicle (1,2-propanediol, n=8 or 10), OCA (50 mg/kg, n=10 or 11), or DY268 (10 mg/kg, n=8) twice a day for three days via oral gavage. Liver samples were collected on treatment day three at the 2 pm time frame and snapped frozen in liquid nitrogen. These studies were approved by the Institutional Animal Care and Use Committee (IACUC) of the University of Rhode Island.

Long-term mouse HCC models

As reported and demonstrated in our laboratory, FXR-KO mice spontaneously developed HCC tumor at the age of 13-15 months on a regular diet [6, 10]. FXR-KO mice at the age of 2-3 months were hydrodynamically injected with USP2b expression construct plasmid DNA at a dose of 0.5 μg/g via tail vein. Control mice received no treatment or empty expression vector. All mice were on a regular chow diet. At the age of 13-15 months, the mice were euthanized. Body and liver weights were recorded. Visible tumors in the liver were counted, and the tumor sizes were measured.

5' rapid amplification of cDNA ends (5'RACE)

Nuclear RNA was extracted from liver tissues using the Sureprep Nuclear/Cytoplasmic RNA Purification kit from Fisher Scientific (catalog #BP2805-50). Nuclear RNA was utilized to detect transcription starting sites (TSS) following the 5'RACE kit protocol which was purchased from Thermo Fisher Scientific (catalog #18374058). The USP2b gene specific primers (GSP) used for cDNA synthesis and PCR amplification were purchased from Gene Universal (primers listed on **Table 1**). GSP1 and 2 were used for cDNA synthesis, and GSP3, 4, and 5 were used for the nested PCR. It should be mentioned that all the primers are in the first intron of USP2b to make sure that only the pre-mRNAs were amplified. PCR products were isolated and subjected to sequencing by the Rhode Island Genomics and Sequencing Center (RIGSC).

Transfection and treatments of Huh 7 cells

Huh 7 cells seeded in 6-well plates were transfected with 2 μg of pcDNA, FXRα1, or FXRα2 for 16 hours followed by treatment with vehicle (0.1% DMSO), FXR agonist OCA (1 μm or 5 μm), FXR agonist GW4064 (1 μm), or FXR antagonist DY268 (1 μm) for 30 hours. At the end of the treatment, cells were lysed and cell lysates were collected for protein detection and total RNA extraction for mRNA quantification as described before [24, 25].

Real-time quantitative reverse transcription PCR (RT-qPCR)

Total RNA isolation from Huh 7 cells or liver tissues, cDNA synthesis and TaqMan real-time PCR assays were performed as previously described [24, 25]. TaqMan PCR probes including human USP2b (catalog#: Hs01592505_m1), small heterodimer partner (SHP) (catalog#: Hs00222677_m1) and glyceraldehyde 3-phosphate dehydrogenase (GAPDH) (catalog#: 435-

2665), mouse USP2b probes (catalog#: Mm-01168648) and mouse GAPDH probes (catalog#: 4352661) were purchased from Thermo Fisher Scientific.

Western blot analysis

Total protein was extracted from Huh 7 cells or liver tissues using RIPA lysis buffer for protein detection via western blot as published previously [9, 26, 27]. Primary goat anti-USP2 total (AF5804, R & D Systems) and secondary rabbit anti-goat IgG (H+L) HRP antibodies (catalog #81-1620, Thermo Fisher Scientific) were used. Protein bands were quantified with Image J.

Dual-luciferase reporter assays

The dual-luciferase reporter assays were performed as reported before [23, 24]. Briefly, Huh 7 cells seeded in 24-well plates were transfected with 100 ng of pUSP2b (-1.5 kb) promoter reporter or FXRE reporter constructs, 100 ng of FXRα1, FXRα2 or pcDNA vector as control, followed by treatment of transfected cells with FXR agonist OCA (5 μm) or vehicle for 30 hours. Cells were lysed with the passive lysis buffer. The dual-luciferase reporter assays were carried out with cell lysates according to the protocol provided by the manufacturer. The firefly luminescence was normalized based on the Renilla luminescence signal, and the ratio of treatment over control served as fold activation. Data is presented as mean ± standard deviation of at least three separate experiments.

Electrophoretic mobility shift assay (EMSA)

To test FXR's direct binding to the FXRE in the USP2b promoter *in vitro*, nuclear protein extracts of Huh7 cells transfected with FXRα2 were collected using the NE-PER™ Nuclear and Cytoplasmic Extraction Kit from Thermo Fisher Scientific (catalog #78833). EMSA was performed using the LightShift Chemiluminescent EMSA Kit purchased from Thermo Fisher Scientific (catalog #20148) as described [9, 26]. The sense and antisense oligonucleotide probes containing the USP2b-FXRE were 5' end biotin-labeled and synthesized by Gene Universal. To establish the specificity of the binding, competition assays were conducted by incubation of nuclear proteins and biotin-labeled probe with 40X unlabeled or mutated USP2b-FXRE. The sequences of the FXRE probe and FXRE mutant were listed in **Table 1**. To determine whether FXR is a component of the protein complex binding to the probe, supershift assays were performed using antibodies against human FXR (catalog #sc-25309, Santa Cruz Biotechnology). Non-immune mouse IgG (sc-2025, Santa Cruz Biotechnology) was included as a negative control. For the supershift assays, antibodies were incubated with nuclear extracts at 4°C for 40 min before adding the biotin-labeled probe. The protein-DNA complexes were resolved in a 6.5% native polyacrylamide gel, transferred to nylon membranes, and detected by chemiluminescence according to the EMSA protocol provided by the manufacturer.

Chromatin immunoprecipitation (ChIP) and ChIP-qPCR

Huh 7 cells in 6-well plates were transfected with 2 μg of FXRα2 plasmid DNA for 16 hours, followed by treatment with DMSO (0.1% v/v) or OCA treatment (1 μm) for 30 hours. Liver tissues from mice treated with OCA (50 mg/kg, twice a day for three days via oral gavage) or vehicle were also used for ChIP assays. Chromatins were prepared from transfected Huh 7 cells or mouse liver tissues as described previously [9, 25]. A fraction of chromatins (5 μg) was immunoprecipitated with 2 μg of anti-FXR antibodies (catalog #sc-25309, Santa Cruz Biotechnology), anti-RNA polymerase II antibodies as the positive control, and non-immune IgG as the negative control, which were purchased with the Epigentek ChIP system (catalog #P-2027-48). ChIP assays were performed following the Epigentek ChIP protocol. Chromatin immunoprecipitated DNA was quantified with the SYBR green qPCR kit (catalog #A25742, Thermo Fisher Scientific). Human and mouse USP2b specific primers flanking the FXRE were used for ChIP-qPCR (**Table 1**). To determine coregulator recruitment within the USP2b promoter regions upon FXR activation, chromatins were immunoprecipitated with antibodies against nuclear corepressor (NCoR) (catalog #sc-8994, Santa Cruz Biotechnology), steroid receptor coactivator 1 (SRC-1) (catalog #sc-6096, Santa Cruz Biotechnology), glucocorticoid receptor interacting protein 1 (GRIP-1) (catalog #sc-8996, Santa Cruz Biotechnology), co-activator-associated arginine methyltransferase 1 (CARM-1) (catalog #33176, Santa Cruz

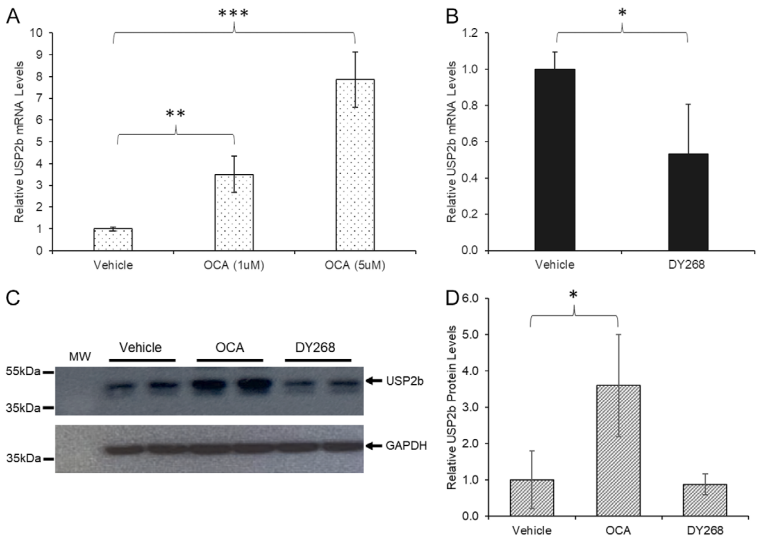

Figure 1. The effects of FXR agonist and antagonist treatment on USP2b expression *in vitro* in Huh 7 cells. Huh 7 cells seeded in 6-well plates were treated with (A) FXR agonist OCA at two doses (1 μm and 5 μM) and vehicle or (B) with FXR antagonist DY268 (1 μM) and vehicle for 30 hours, followed by quantification of USP2b mRNA levels with real-time PCR. (C) USP2b protein expression detected by Western blot, following treatments of Huh 7 cells with FXR agonist and antagonist as described in (A and B). (D) Quantification USP2b protein levels showed in (C). *P<0.05, **P<0.01, ***P<0.001 in Student's t-test for pair-wise comparison or one-way ANOVA, followed by Tukey post-hoc test for multiple group comparisons.

Biotechnology), and peroxisome proliferator-activated receptor-gamma coactivator-1alpha (PGC-1α) (catalog #sc-5815, Santa Cruz Biotechnology), followed by ChIP-qPCR as described above.

Statistical analysis

Student t-test was applied to pair-wise comparison for normally distributed data. One-way ANOVA was applied to analyze data with multiple groups, followed by Tukey post-hoc test for multiple comparisons. Non-parametric Mann-Whitney U test was performed for data with non-normal distribution. Tukey's Fence was used to detect outliers. A *p*-value of 0.05 or lower was considered statistically significant.

Results

USP2b expression was upregulated by FXR activation and downregulated by FXR antagonism in vitro in Huh 7 cells

Our previous study showed that USP2b expression levels were significantly reduced [23] while FXR signaling was dysregulated in HCC subjects [9]. To determine whether USP2b is regulated by the FXR signaling, Huh 7 cells were treated with FXR agonist OCA or antagonist DY268, followed by detection of USP2b mRNA by real-time PCR and protein by Western blot. As shown in **Figure 1A**, OCA dose-dependently induced USP2b mRNA expression (P<0.01 and P< 0.001). On the other hand, DY268 significantly reduced USP2b mRNA expression (P< 0.05) (**Figure 1B**). Consistently, USP2b protein levels were markedly increased in the cells treated with OCA (P< 0.05) while treatment with DY268 had limited effects on USP2b protein levels (**Figure 1C** and **1D**). Taken together, activation of FXR significantly increased USP2b expression at both mRNA and protein levels while antagonizing FXR reduced USP2b mRNA but not protein levels. The results demonstrated that FXR signaling regulated USP2b expression *in vitro* in Huh 7 cells.

FXR regulated USP2b expression in vivo in mice

To substantiate the findings from Huh 7 cells, we treated the mice with FXR agonist OCA or FXR antagonist DY268, followed by measuring the mRNA and protein levels of USP2b. As shown in **Figure 2A**, OCA treatment markedly induced USP2b mRNA (P<0.001). On the other hand, treatment with FXR antagonist DY268 significantly down-regulated USP2b mRNA expression (P<0.05) (**Figure 2C**). Serving as positive control, SHP mRNA expression was significantly up- and down-regulated by OCA (**Figure 2B**) and DY268 (**Figure 2D**), respectively. Consistent with the mRNA levels, USP2b protein levels were significantly induced by OCA (**Figure 2E** and **2F**) while DY268 treatment significantly reduced USP2b protein abundances (**Figure 2G** and **2H**). The data convincingly demonstrated that USP2b is transcriptionally regulated by the FXR signaling pathway *in vivo*.

To confirm the results, we tested the effects of FXR knockout on USP2b expression. We hypothesized that USP2b expression was minimally affected by FXR agonist or antagonist in

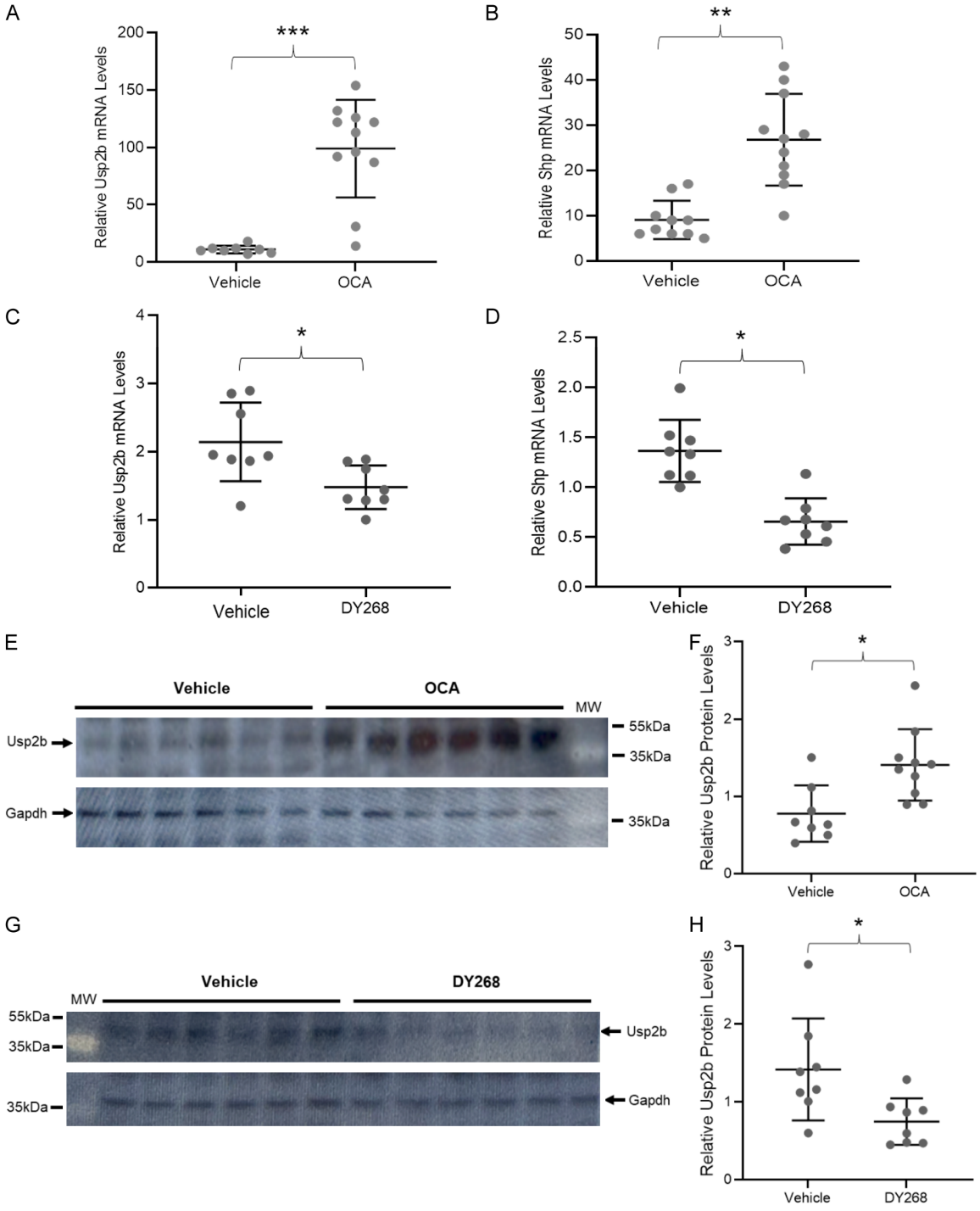

Figure 2. The effects of FXR activation and antagonism on USP2b expression *in vivo* in mice. C57BL/6J wt mice were treated with OCA (50 mg/kg) (n=11), DY268 (10 mg/kg) (n=8) and vehicle (n=8) twice a day for three days via oral gavage, followed by quantification of USP2b mRNA and protein levels. (A) The mRNA levels of USP2b and (B) FXR target gene SHP, following FXR activation with OCA. (C) The mRNA levels of USP2b and (D) SHP, following treatment of FXR antagonist DY268. (E) USP2b protein detected by Western blot and (F) quantification of the USP2b protein levels showed in (E), following treatment with FXR agonist OCA or vehicle. (G) USP2b protein detected by Western blot and (H) quantification of USP2b protein levels following treatment with FXR antagonist DY268. *P<0.05, **P<0.01, ***P<0.001 with Student's t-test.

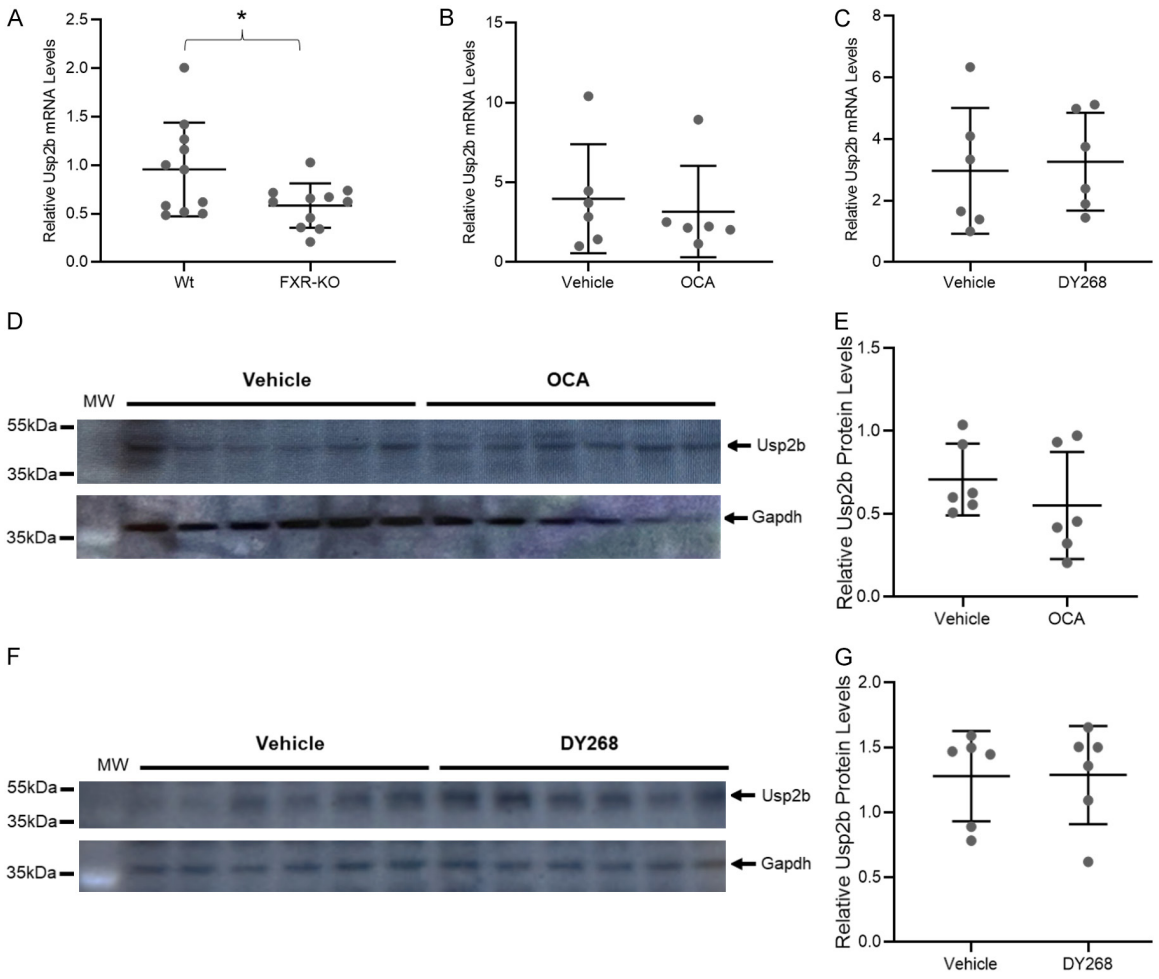

Figure 3. USP2b expression in FXR-KO mice. (A) USP2b mRNA expression levels in wt and FXR-KO mice. (B) FXR-KO mice were treated with FXR agonist OCA (50 mg/kg) and vehicle or (C) with FXR antagonist DY268 (10 mg/kg) and vehicle twice a day for three days via oral gavage, followed by quantification of USP2b mRNA levels by real-time PCR. (D) USP2b protein detected by Western blot and (E) quantification of USP2b protein levels following treatment with FXR agonist OCA. (F) USP2b protein detected by Western blot and (G) quantification of USP2b protein levels following treatment with FXR antagonist DY268. *P<0.05 with Student's t-test.

the absence of FXR. As shown in **Figure 3A**, USP2b mRNA expression was significantly reduced in FXR knockout (FXR-KO) mice when compared with wt mice, consistent with the notion that FXR activation induces USP2b expression. More convincingly, knockout of FXR completely blunted the effects of FXR agonist OCA and antagonist DY268 on USP2b expression. As shown in **Figure 3B**, USP2b mRNA expression levels were comparable in mice treated with OCA or vehicle. Similarly, USP2b mRNA expression was not affected by DY268 treatment (**Figure 3C**). Consistent with USP2b mRNA expression, USP2b protein abundances were minimally altered in mice treated with OCA (**Figure 3D** and **3E**) or DY268 (**Figure 3F** and **3G**) when compared to corresponding vehicle controls. The data thus fully established that USP2b was transcriptionally regulated by the FXR signaling pathway and USP2b is a downstream target of FXR pathway.

Isoform-specific transcriptional regulation of USP2b by FXR

There are two FXR isoforms in the liver, including FXRα1 and FXRα2. To determine whether USP2b is regulated by FXRα1, FXRα2 or both, Huh 7 cells were transfected with FXRα1, FXRα2 or pcDNA vector as control, followed by treating the transfected cells with two doses of FXR agonist OCA or vehicle. As shown in **Figure 4A**, low levels of USP2b mRNA induction, 3.5 and 7.5-fold, were detected in cells transfected

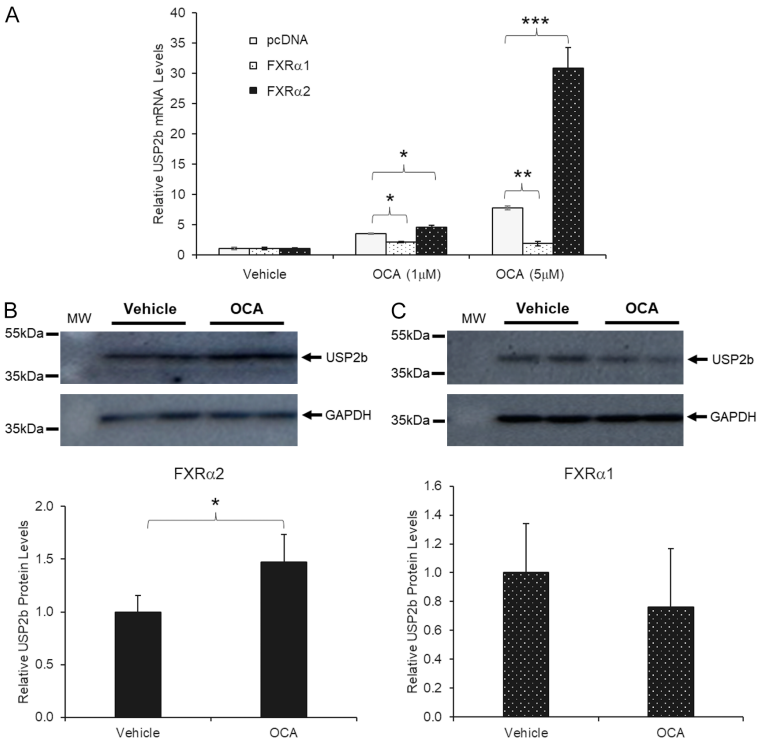

Figure 4. Isoform-specific upregulation of USP2b expression by FXR. Huh 7 cells seeded in 6-well plates were transfected with FXRα1, FXRα2 or empty vector (pcDNA) for 16 hours followed by treatment with OCA at two doses (1 and 5 μm) and vehicle for 30 hours. (A) USP2b mRNA levels were quantified by real-time PCR. (B) USP2b protein levels detected by Western blot in the cells transfected FXRα2 or (C) FXRα1, following treatment with OCA (5 μM) or vehicle. *P<0.05 with Student's t-test.

with pcDNA vector and treated with 1 and 5 μM OCA, respectively. Such low levels of induction are most likely due to activation of the endogenous FXRα1 and FXRα2 in Huh 7 cells. When the cells were transfected with FXRα2, USP2b mRNA expression was dose-dependently and potently induced by OCA. The USP2b mRNA levels increased by 4.5 and 30.8-fold in cells treated with 1 and 5 μM OCA, respectively. However, when the cells were transfected with FXRα1, the expression levels of USP2b mRNA were minimally induced by OCA, increasing 2.1 and 1.8-fold in cells treated with 1 and 5 μM OCA, respectively. Furthermore, when compared to the cells transfected with pcDNA vector control, the expression levels of USP2b mRNA in cells transfected with FXRα1 were significantly reduced (P<0.05).

Consistent with mRNA levels, USP2b protein expression levels were significantly upregulated in cells transfected with FXRα2 in the presence of 5 μM OCA (**Figure 4B**). In contrast, USP2b protein expression levels were notably reduced in cells transfected with FXRα1 in the presence of 5 μM OCA (**Figure 4C**). Taken together, the data demonstrated that USP2b was transcriptionally upregulated by FXRα2 signaling pathway while FXRα1 may act as a competitor or repressor to interfere FXRα2-mediated transcriptional regulation of USP2b.

Transactivation of USP2b promoter by FXR signaling

To further dissect the transcriptional regulation of USP2b by FXR signaling, the tentative USP2b promoter was cloned into a luciferase reporter and characterized. It was speculated that USP2 isoforms including USP2a and USP2b were transcribed from a single promoter and derived from alternative splicing of the pre-mRNA [23]. However, in our previous studies, we revealed an opposite trend of USP2a and USP2b expressions in human and mouse HCC tumor tissues [23, 24]. USP2a expression was upregulated while USP2b expression was significantly downregulated. We also found that USP2b expression exhibited a robust circadian pattern while USP2a expression showed limited fluctuation during a 24-hour period (**Figure 5**), which is in line with a previous report [28]. The differential expression characteristics of these two isoforms suggest a potential for two separate promoters directing USP2a and USP2b transcription. Indeed, bioinformatic analysis predicted USP2a and USP2b to display alternative promoters [29]. To confirm such prediction, 5'RACE was performed using nuclear pre-mRNA isolated from mouse liver tissues and primers designed within the 1st intron of the pre-mRNA. The resulting PCR products were subjected to nucleotide sequence analysis to uncover the transcription starting sites (TSS) of USP2a and USP2b. As shown in **Figure 6A**, the TSS for USP2a and

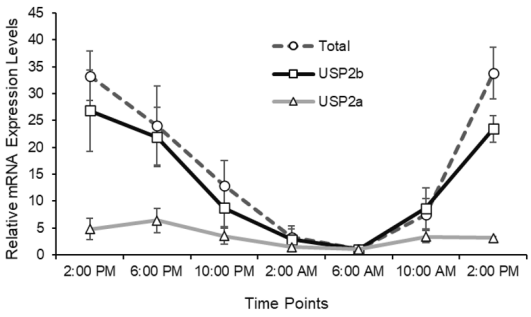

Figure 5. Distinct circadian patterns of USP2a and USP2b. The USP2a, USP2b and USP2 total mRNA levels were detected and quantified with real-time PCR using isoform-specific primers at 6 time points (every 4 hours during a 24-hour period, N=4/time).

USP2b was different, more specifically, USP2b TSS is located approximately 18 kb downstream the USP2a TSS. The data thus confirmed that USP2a and USP2b expression are under the control of two independent promoters.

To functionally characterize the USP2b promoter, a 1.5 kb promoter region upstream USP2b TSS was cloned into the pGL3 luciferase reporter vector, resulting in pGL3-USP2b (-1.5 kb) reporter construct. As shown in **Figure 6B**, similar to the cells receiving negative pcDNA control, treatment with FXR agonists OCA and GW4064 did not induce USP2b promoter activities in cells transfected with FXRα1. However, in the cells transfected with FXRα2, the basal USP2b promoter activity was significantly increased. More importantly, treatment with OCA and GW4064 significantly induced USP2b promoter activities. The data thus demonstrated that activation of FXRα2 but not FXRα1 induced transactivation of USP2b promoter. Indeed, the ratios of FXRα1 and FXRα2 dictated the transactivation of the USP2b promoter. As the ratios of FXRα2 decreased from 100% to 0%, the USP2b promoter transactivation levels were gradually reduced in the absence or presence of FXR agonist OCA (**Figure 6C**). The results are consistent with the FXRα2-specific regulation of USP2b expression at mRNA and protein levels (**Figure 4**).

Identification of the functional FXR response element (FXRE) in the USP2b promoter

To map the FXRE in the USP2b promoter, the genomic sequence of the 1.5 kb fragment upstream the TSS of USP2b was bioinformatically analyzed with three software PROMO, NUBIScan, and MatInspector. The predicted FXRE that was commonly predicted by the three software was selected to test its activities. Within the USP2b promoter, one such FXRE was identified at the nucleotide sequence -1.353 to -1.314 kb (**Figure 7A**). The predicted FXRE sequence (AGGTCGCTGCAGT) is 62% conserved with the IR1 FXRE consensus sequence. To functionally test the FXRE, three repeats of the FXRE wild type and FXRE mutant were cloned into the pGL3p element reporter vector, resulting in phUSP2b-FXRE and phUSP2b-FXRE-mut reporter constructs, followed by characterization of the reporters with luciferase assays in the presence of FXRα2 and its agonist OCA. As shown in **Figure 7B**, FXR activation by OCA significantly increased luciferase activities of the FXRE reporter while minimal activities were detected in the cells transfected with FXRE-Mut. The data thus confirmed the functionality of FXRE in the USP2b promoter.

FXRα2 specifically binds to the FXRE of USP2b promoter in vitro

To confirm the direct binding of FXRα2 to the identified FXRE in the USP2b promoter, two series of EMSAs were performed with 5' end biotin-labeled USP2b-FXRE oligonucleotides as the DNA probes containing the predicted FXREs (oligonucleotides listed on **Table 1**) and nuclear protein extracts from FXRα2-transfected Huh 7 cells. As shown in **Figure 7C**, when USP2b-FXRE probes were incubated with nuclear extract containing FXRα2 protein, a single dominant shifted band was displayed. The shifted band was completely outcompeted by 40× unlabeled wt FXRE oligonucleotides but not by the 40× mutated FXRE oligonucleotides, indicating the specific binding of the FXRE probe with a cellular protein. To determine whether the shifted band resulted from FXR's binding to the FXRE probe, super-shift assays were performed with antibodies against FXR. Preincubation with FXR antibodies and nuclear FXR extracts resulted in complete disappearance of the shifted band, suggesting that the binding of FXR antibodies to FXR protein interferes with its binding to the FXRE probe. On the other hand, preincubation with IgG antibodies as negative control sustained the DNA/protein complex formed, indicating

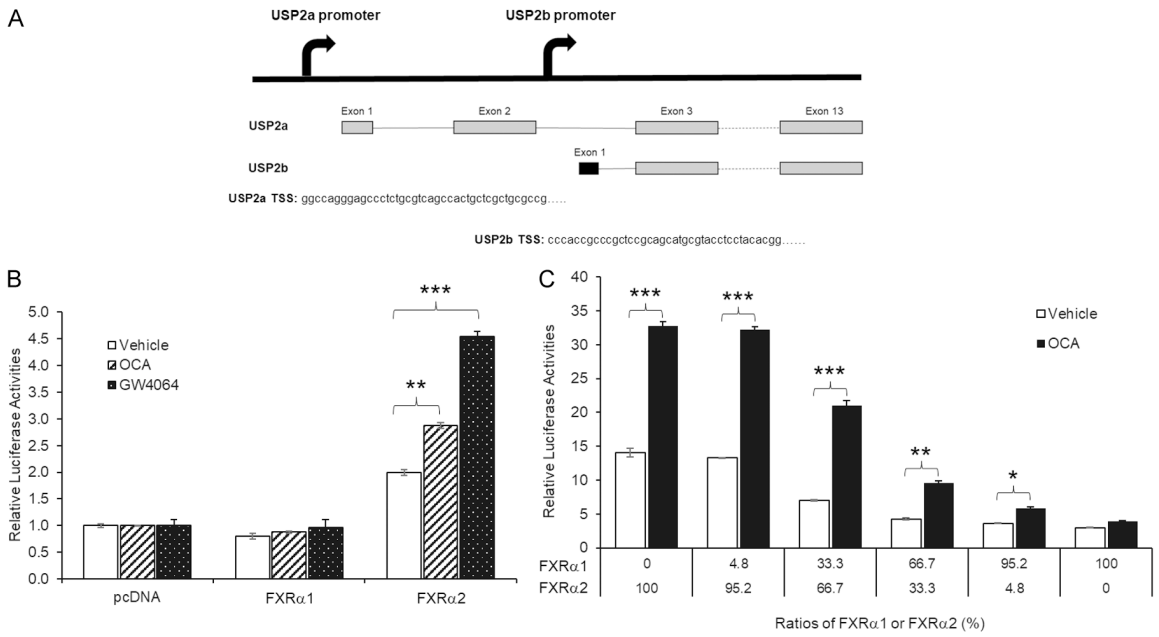

Figure 6. Identification of USP2b promoter and its transactivation by FXR. A. The transcription starting sites (TSS) for USP2a and USP2b were identified by 5'RACE. Liver tissues were used to isolate pre-mRNA from hepatocyte nuclei, followed by PCR amplification and sequencing of the TSS. B. Huh 7 cells were co-transfected USP2b promoter reporter with FXRα1, FXRα2 or empty pcDNA vector, followed by treatment of the cells with OCA (5 μM), GW4064 (1 μM) or vehicle for 30 hours and subsequent detection of luciferase activities in the dual luciferase assays. C. Huh 7 cells were transfected with FXRα1 and FXRα2 in a series of ratios from 0% to 100%, followed by treatment of the cells with OCA (5 μM) or vehicle for 30 hours and subsequent detection of luciferase activities. *P<0.05, **P<0.01, ***P<0.001 with Student's t-test or one-way ANOVA, followed by Tukey post-hoc test.

that the IgG antibody does not interfere FXRα2 binding to the USP2b-FXRE probe. On the other hand, it was noted that there was a new shifted band with smaller size with IgG antibodies. This shifted band most likely resulted from non-specific binding of a protein in the IgG preparation to the FXRE probe. Taken together, the data demonstrated that FXRα2 specifically bound to the FXRE in the USP2b promoter.

FXR was recruited to the FXRE of USP2b promoter in vivo and in intact cells

A series of ChIP assays were carried out to determine whether FXR is specifically recruited to the FXRE of the USP2b promoter. First, to determine whether FXR is enriched in the FXRE of USP2b promoter in human liver, chromatins were prepared from human liver tissues, followed by immunoprecipitation with antibodies against human FXR, RNA polymerase II as positive control and non-immune IgG as negative control. As shown in **Figure 8A**, FXR recruitment to the FXRE of USP2b promoter was significantly enriched when compared with non-immune IgG control. As expected, RNA polymerase II was also robustly recruited to the USP2b promoter. The data thus demonstrated that FXR was enriched in the FXRE of USP2b promoter in human liver tissues.

We next performed ChIP assays to determine whether FXR's recruitment to the FXRE of USP2b promoter was increased upon FXR activation *in vitro* in Huh 7 cells and *in vivo* in mice. For the *in vitro* study, Huh 7 cells were transfected with FXRα2 for 16 hours, followed by treatment with DMSO or OCA for 30 hours. Chromatin was extracted from these cells and immunoprecipitated with antibodies against FXR and RNA polymerase II, and non-immune IgG antibodies. As shown in **Figure 8B**, FXR and RNA polymerase II's recruitment to the FXRE of USP2b promoter were significantly increased upon FXR activation by OCA when compared to the vehicle treatment while minimal changes were detected with the non-immune IgG.

For the *in vivo* study, mice were treated with vehicle or OCA (50 mg/kg) twice a day for three days, and liver samples were collected on day three. Chromatin was extracted from liver tis-

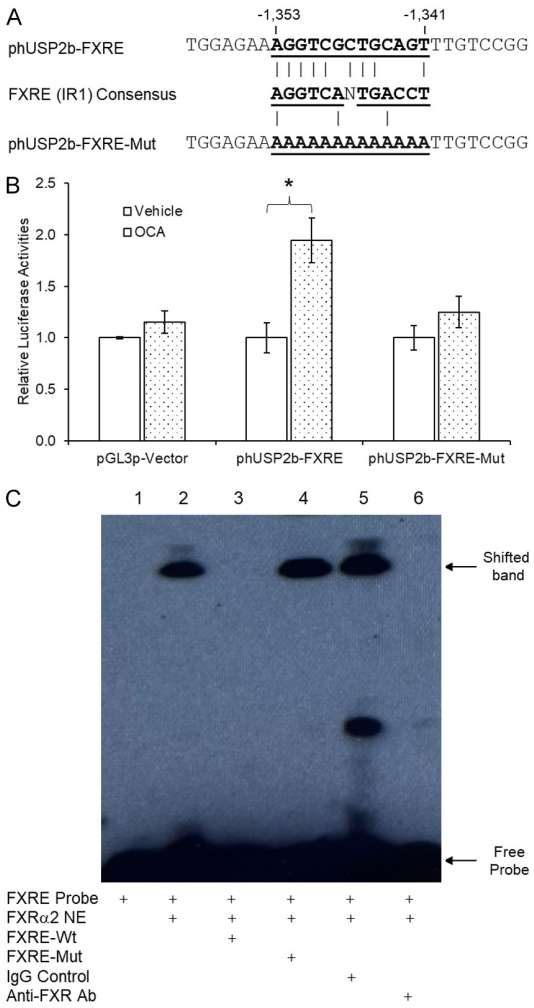

Figure 7. Identification and functional characterization of the FXRE in the USP2b promoter. A. The sequence and location of the FXRE in the USP2b promoter. Three copies of the FXRE and its mutant were cloned into the pGL3-Promoter (pGL3p) vector, resulting in two element reporter constructs phUSP2b-FXRE and phUSP2b-FXRE-Mut. B. Huh 7 cells seeded in 24-well plates were co-transfected phUSP2b-FXRE, phUSP2b-FXRE-Mut or pGL3p-vector with FXRα2, followed by treatment of the transfected cells with OCA (5 μM) for 30 h and subsequent detection of luciferase activities in the dual luciferase assays. C. Electrophoretic mobility shift assays (EMSA) were carried out using biotin labeled FXRE as probe and nuclear extract isolated from Huh 7 cells overexpressing FXRα2. *P<0.05 with Student's t-test.

sues and immunoprecipitated with anti-FXR, anti-RNA polymerase II antibodies, and non-immune IgG as negative controls. As shown in **Figure 8C**, there was a significant increase in FXR and RNA-polymerase II recruitment in the USP2b promoters upon FXR activation by OCA when compared to vehicle treatment. On the other hand, there were no changes in FXR and RNA polymerase II recruitment detected with non-immune IgG. Taken together, the consistent data from *in vitro* in Huh 7 cells and *in vivo* in mice demonstrated that FXR was specifically and increasingly recruited to the FXRE of the USP2b promoter upon FXR activation, leading to increased transcription of the USP2b by FXR signaling.

The recruitment dynamics of FXR co-regulators to the FXRE of USP2b promoters following FXR activation

Studies have demonstrated that transcriptional coactivators such as SRC-1 [30], GRIP-1 [31], CARM-1 [32] and PGC-1α [33] are recruited with ligand-activation of FXR. On the other hand, NcoR is associated with FXR signaling [34]. To investigate the recruitment dynamics of FXR co-regulators to the human USP2b promoter following FXR activation, Huh 7 cells were treated with FXR agonist OCA or vehicle as control, followed by performing the quantitative ChIP assays for those co-regulators. As shown in **Figure 9A**, there was a significant increase in CARM-1 recruitment to the human USP2b promoter regions when compared to vehicle treatment. As expected, RNA polymerase II recruitment to the region was also significantly increased. Minimal changes were detected upon FXR activation for SRC-1. The recruitment of three other co-regulators, including NcoR, GRIP-1 and PGC-1α, was reduced but without reaching statistical significance. As expected, no changes were detected by the non-immune IgG. The results thus established that CARM-1 was the major co-activator recruited to the human USP2b promoter upon FXR activation, leading to increased human USP2b transcription.

To investigate the recruitment dynamics of FXR co-regulators to the mouse USP2b promoter following FXR activation, mice were treated with FXR agonist OCA or vehicle. Chromatin was extracted from mouse liver tissues and immunoprecipitated with antibodies against corepressor NCoR, and coactivators SRC-1, GRIP-1, CARM-1, and PGC-1α along with anti-RNA polymerase II as a positive control and non-immune IgG as a negative control. As shown in **Figure 9B**, coactivators GRIP-1 and PGC-1α were significantly recruited to the mouse USP2b pro-

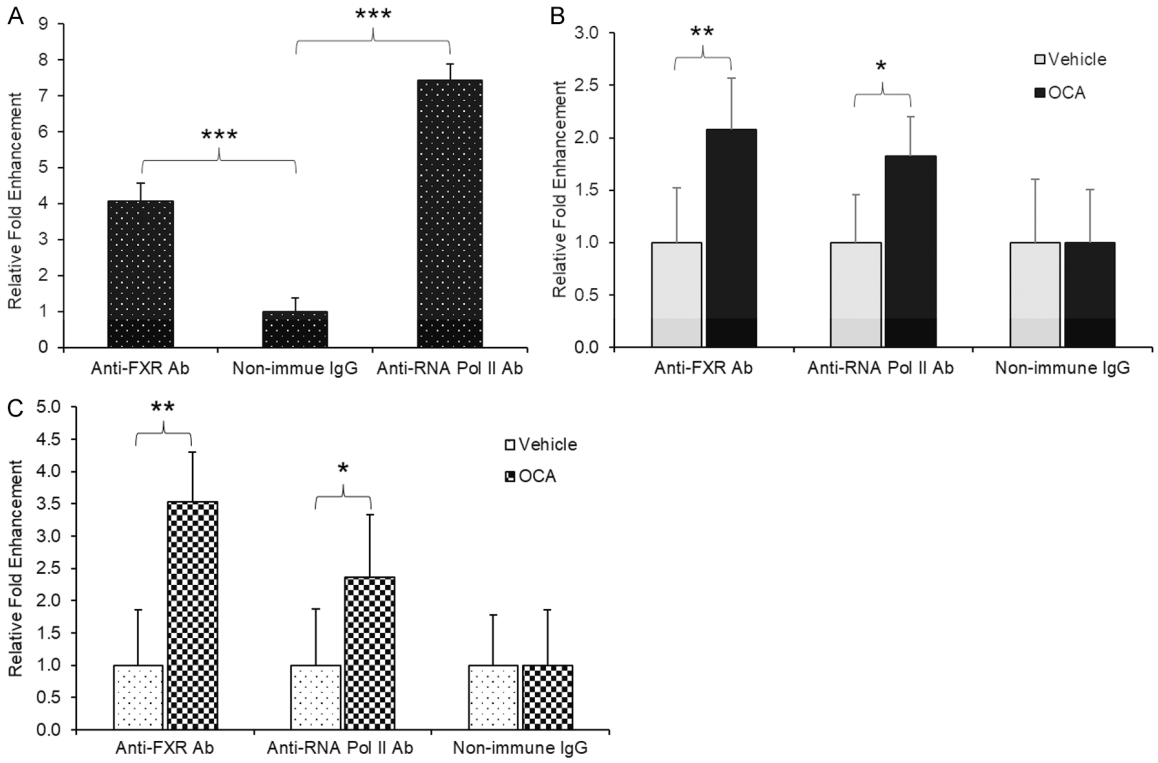

Figure 8. FXR recruitment to the FXRE of USP2b promoter *in vivo* and in intact cells. A. ChIP-PCR assays were carried out using chromatins isolated from human liver tissues and antibodies against FXR and RNA polymerase II (as positive control) and non-immune IgG (as negative control). B. Huh7 cells were transfected with FXRα2 for 16 hours, followed by treatment with DMSO or OCA for 30 hours. Chromatin was extracted from the transfected cells and immunoprecipitated with antibodies against FXR and RNA polymerase II, and non-immune IgG antibodies, followed by ChIP-PCR assays. C. Mice were treated with vehicle (n=6) or OCA (n=6) (50 mg/kg) twice a day for three days, and liver tissues were collected on day three. Chromatin was extracted from liver tissues and immunoprecipitated with anti-FXR, anti-RNA polymerase II antibodies, and non-immune IgG, followed by the ChIP-PCR assays. *P<0.05, **P<0.01, ***P<0.001 with Student's t-test for pair comparison or one-way ANOVA, followed by Tukey post-hoc test for multiple group comparison.

moter upon FXR activation. As expected, RNA polymerase II recruitment was also significantly increased, while no changes were detected by the non-immune IgG. Taken together, the results established that coactivators GRIP-1 and PGC-1α were the major coactivators recruited to the mouse USP2b promoter upon FXR activation, responsible for transcriptional enhancement of mouse USP2b following FXR activation.

The effects of exogenously expressed USP2b on the development of HCC in FXR-KO mice

Our current study demonstrated that USP2b was transcriptionally regulated by the FXR signaling. Activation of FXR significantly upregulated USP2b expression. The findings are consistent with our previous results that HCC subjects had reduced or totally absent FXR expression [9] with concurrently reduced USP2b expression [23]. It is well established by others and demonstrated in our laboratory that FXR-KO mice spontaneously develop HCC as they age at 13-15 months [6, 23, 24]. To determine whether the reduced USP2b expression in FXR-KO mice contributes to the pathogenesis of HCC, FXR-KO mice were given USP2b expression construct hydrodynamically at young age. Control FXR-KO mice received no treatment or empty expression vector. HCC development was assessed at the age of 13-15 months. As shown in **Figure 10A**, there were no differences in body weight between the two groups. However, the average liver weight was significantly reduced from 2.5±0.7 g in control mice to 1.9±0.5 g in the USP2b-treated mice (P< 0.05) (**Figure 10B**). Consequently, the liver/body weight ratios were significantly reduced

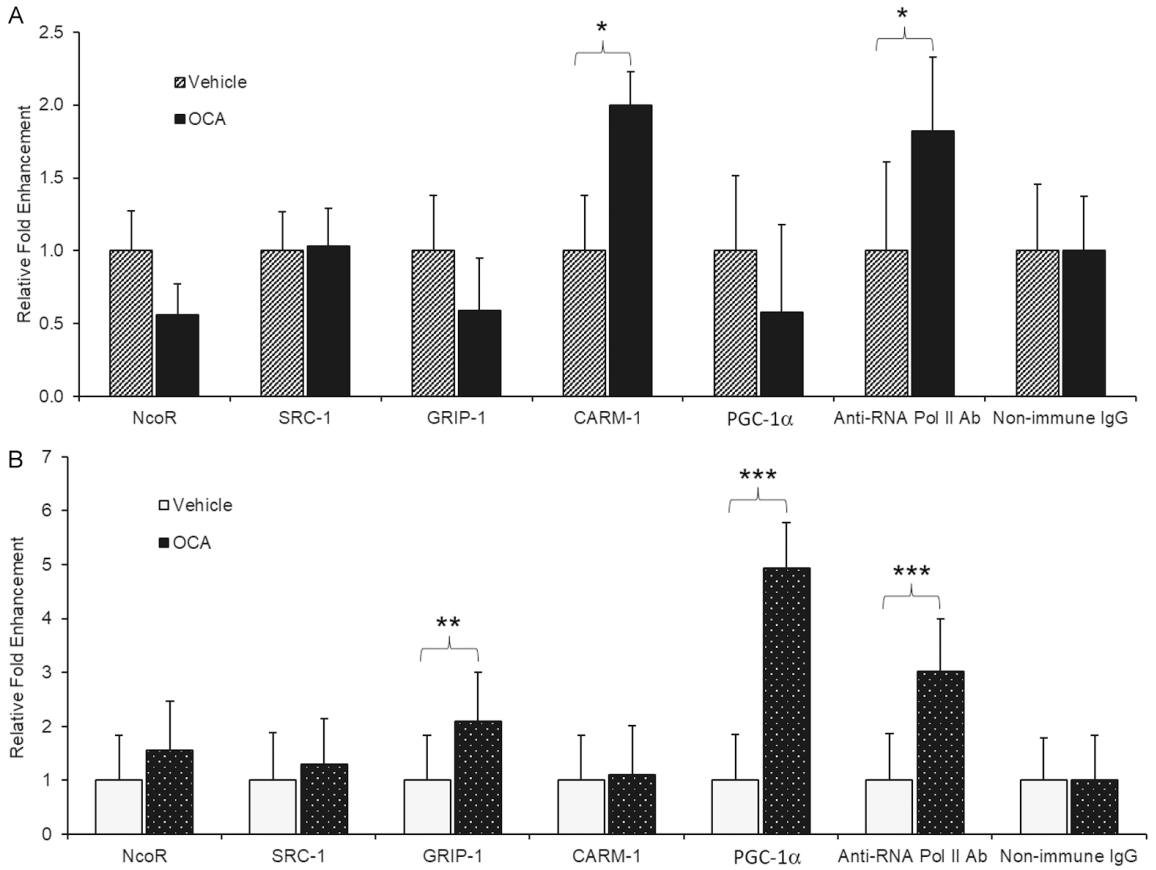

Figure 9. Recruitment of FXR coregulators to the FXRE of USP2b promoter upon FXR activation. A. Huh7 cells were transfected with FXRα2, followed by treatment with vehicle DMSO or OCA for 30 hours. B. Mice were treated with vehicle or OCA (50 mg/kg) via oral gavage for 3 days and liver tissues were collected. Chromatins were prepared from Huh 7 cells and mouse liver tissues and immunoprecipitated with antibodies against FXR coregulators including NcoR, SRC-1, GRIP-1, CARM-1 and PGC-1α and RNA polymerase II as positive control and non-immune IgG as negative control. *P<0.05, **P<0.01, ****P<0.001 with Student's t-test.

from 0.078±0.024 in control mice to 0.060± 0.008 in the USP2b-treated mice (P<0.05) (**Figure 10C**). USP2b overexpression decreased the percentages of mice developed tumors from 94.7% in control to 85.7% in USP2b-treated mice without reaching a statistical significance (**Figure 10D**). Tumor size measurements revealed that the average tumor size was significantly reduced in USP2b-treated mice when compared to control mice (P<0.001) (**Figure 10E** and **10G**) while the numbers of tumors in each tumor-bearing mouse were comparable in both groups (**Figure 10F** and **10G**). Taken together, exogenous overexpression of USP2b in FXR-KO mice significantly reduced liver weight and tumor size with limited effects on tumor numbers, consistent with its tumor suppressive activity.

Discussion

Previous studies have demonstrated that both FXR and USP2b are dysregulated in HCC [9, 23, 35-37]. The expression levels of FXR were largely downregulated and such downregulation was negatively correlated with the malignancy grade of HCC [35-37]. Our previous study also found that USP2b expression was significantly downregulated in HCC tumor when compared to normal healthy liver tissues [23]. However, the molecular linkage between FXR dysregulation and reduced USP2b expression in HCC is unknown. In this study, we discovered that FXR transcriptionally regulated USP2b expression. Activation or antagonizing of FXR signaling potently upregulated or down-regulated USP2b expres-

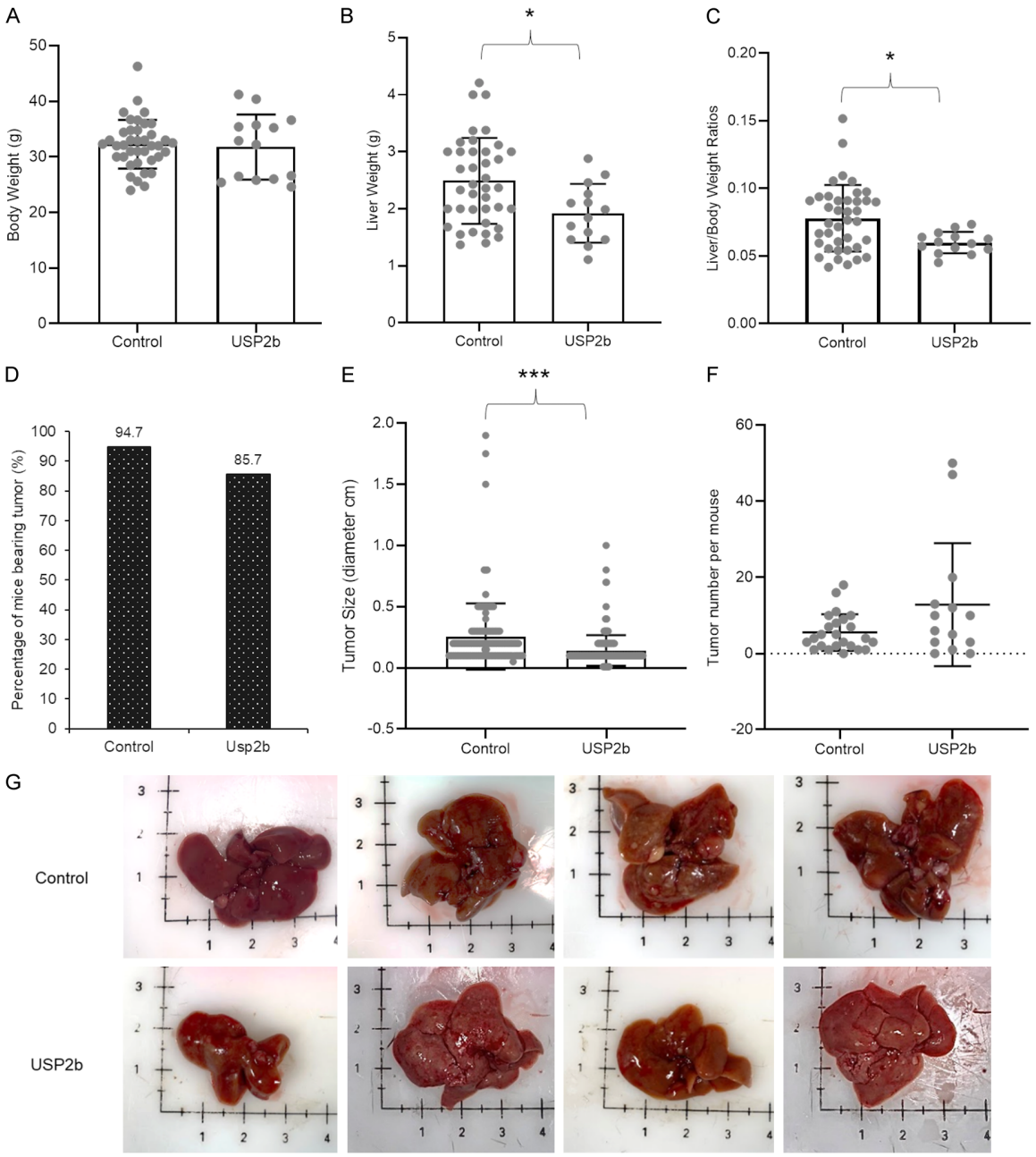

Figure 10. The effects of exogenous overexpression of USP2b on the development of HCC in FXR-KO mice. FXR-KO mice at the age of 2-3 months were hydrodynamically injected with USP2b expression construct plasmid DNA at a dose of 0.5 μg/g via tail vein. Control mice received no treatment or empty expression vector. All mice were on a regular chow diet. At the age of 13-15 months, the mice were euthanized. Body and liver weights were recorded. Visible tumors in the liver were counted, and the tumor sizes were measured. (A) body weight, (B) liver weight, (C) liver/body weight ratios, (D) percentages of mice developing visible tumors, (E) tumor sizes, (F) tumor number per mouse and (G) representative livers from control and USP2b-overexpressed group. *P<0.05, ***P<0.001 with Student's t-test for the data in (A-E) and Mann-Whitney U test for the data in (F).

sion, respectively, *in vitro* in Huh 7 cells (**Figure 1**) and *in vivo* in mice (**Figure 2**). Consistently, USP2b mRNA expression was significantly reduced in FXR-KO mice when compared to wt mice (**Figure 3A**). The findings thus established a molecular link between FXR signaling

and USP2b expression and provided an explanation for reduced USP2b expression in HCC as a result of FXR dysregulation.

There are three isoforms of USP2 that have been reported including USP2a, USP2b and USP2c [20-22]. In our previous study, we demonstrated that USP2a and USP2b were expressed in human and mouse liver with USP2b being the predominant isoform whereas USP2c was not detected in both human and mouse liver [23]. It has been speculated that USP2 isoforms are transcribed from a single promoter and derived from alternative splicing of the pre-mRNA [23]. However, in our previous studies, we revealed an opposite trend of USP2a and USP2b expressions in human and mouse HCC tumor tissues [23, 24]. USP2a expression was significantly upregulated while USP2b expression was significantly downregulated. We also found that USP2b expression exhibited a robust circadian pattern while USP2a expression showed limited fluctuation during a 24-hour period (**Figure 5**), which was largely in line with a previous report [28]. The differential expression characteristics of these two isoforms suggest a potential for two separate promoters directing USP2a and USP2b transcription. Indeed, bioinformatic analysis was consistent with this notion and predicted USP2a and USP2b to display alternative promoters [29]. To confirm such prediction, 5'RACE was performed using nuclear pre-mRNA from mouse liver tissues and primers designed within the 1st intron of the pre-mRNA. The results of the 5'RACE revealed that the TSS for USP2a and USP2b are located far apart. More specifically, the USP2b TSS is located approximately 18 kb downstream the USP2a TSS (**Figure 6A**). The data thus confirmed that USP2a and USP2b expression are under the control of two alternative promoters. The identification of a functional FXR response element (FXRE) within the USP2b promoter (**Figure 7**), and the demonstration of direct FXR binding and coactivator recruitment to the region (**Figures 8** and **9**), further validate the USP2b-specific promoter directing USP2b transcription.

With the new findings that USP2a and USP2b are transcribed from alternative promoters, we were able to characterize the USP2b promoter in depth. As shown in **Figure 6B**, transactivation of USP2b promoter is FXR isoform dependent. In the presence of FXRα2, USP2b promoter was potently transactivated by FXR agonists while limited effects were detected in the presence of FXRα1 (**Figure 6B**). The data is consistent with the USP2b expression levels in the presence of FXRα1 or FXRα2 (**Figure 4A**). Treatment with FXR agonist OCA significantly increased USP2b mRNA levels in the presence of FXRα2. However, minimal effects on USP2b mRNA expression were detected by OCA in the presence of FXRα1 (**Figure 4**). Thus, the results firmly established that USP2b was transcriptionally regulated by FXR signaling in an isoform-dependent manner, namely by FXRα2 not FXRα1. Therefore, the relative expression levels of FXRα1 and FXRα2 or the ratio of FXRα1/FXRα2 expression levels dictate the transcriptional expression levels of USP2b (**Figure 6C**). In our previous study, we found that FXR expression was dysregulated in HCC tumors with significantly reduced or totally absence of FXRα2 expression [9]. In other words, the FXR isoform expression was shifted from FXRα2 to FXRα1 in HCC tumors. It is thus reasonably stated that significantly reduced USP2b expression in HCC was, at least in part, a result of FXR dysregulation with reduced FXRα2 expression.

Hydrodynamic injection has been used for transgene expressions *in vivo*, especially in the liver with over 40% hepatocytes expressing the transgenes following a single injection [38, 39]. Several studies have applied the technique to develop animal models for HCC [40-43]. In this study, we used hydrodynamic injection to exogenously overexpress USP2b in FXR-KO mice to determine the effects of increasing USP2b expression on the pathogenesis of HCC. It should be noted that the duration of USP2b overexpression following the hydrodynamic injection is unknown. It has been reported that the durations of transgene expression after hydrodynamic injection greatly vary from a few days to over one year dependent on the promoter and vector backbone [38, 44, 45]. We used pcDNA vector with a CMV promoter driving USP2b expression. It is very likely that high level of USP2b expression is transient with gradually declining expression over time. It is speculated that sustaining high levels of USP2b overexpression would result in more robust effects on the pathogenesis of HCC in FXR-KO mice.

In our *in vivo* study, it should be noted that although the average numbers of tumors in each tumor-bearing mouse were increased

from 5.5±4.8 in control to 12.9±15.8 in USP2b-treated mice, the difference did not reach statistical significance with the nonparametric Mann-Whitney U test (**Figure 10F**). The increased average from the USP2b group was mainly due to the two outlier mice detected by the Tukey's Fence with 47 and 50 tumors, respectively. The reasons for the two outliers having more tumors than the rest of the group remain unknown. We thus concluded that overexpression of USP2b in FXR-KO mice had limited effects on tumor occurrence.

It is well established that FXR acts as a tumor suppressor in HCC development through multiple mechanisms [46-48]. In our previous study, we also found that USP2b exhibited tumor suppressive activities *in vitro* in HepG2 and Huh 7 cells [23]. Overexpression of USP2b in HepG2 and Huh 7 cells significantly enhanced bile acid-induced apoptosis [23]. Consistent with the findings *in vitro*, our *in vivo* study revealed that overexpression of USP2b in FXR-KO mice where USP2b expression was reduced (**Figure 3A**) significantly slowed down tumor growth with reduced tumor sizes (**Figure 10E**). With the identification of USP2b as a downstream target of FXR signaling in this study, we speculate that FXR's ability to exert its tumor suppressive effects is, at least in part, mediated through its target USP2b.

In conclusion, our study reveals a previously unrecognized FXRα2-dependent transcriptional regulation of USP2b, elucidates the distinct promoter architecture of USP2 isoforms, and highlights the functional relevance of USP2b in FXR-deficiency-induced HCC. These findings lay the groundwork for future investigations into isoform-specific FXR modulation of USP2. The interplay between FXR isoforms and USP2b expression suggests that restoring FXRα2 expression and activity or upregulating USP2b expression could represent novel strategies for HCC intervention.

Acknowledgements

This study was supported by the National Institutes of Health (NIH) grants R01CA213 419, R01DK139489 and a predoctoral supplement grant to WA. Additional support for CN was provided by the American Foundation for Pharmaceutical Education (AFPE) Pre-Doctoral Award in Pharmaceutical Sciences. This research was made possible by the use of equipment available through the Rhode Island Institutional Development Award (IDeA) Network of Biomedical Research Excellence from the National Institute of General Medical Sciences of the National Institutes of Health under grant number P20GM103430.

Disclosure of conflict of interest

None.

Abbreviations

5'RACE, 5' rapid amplification of cDNA ends; ATCC, American Type Culture Collection; CARM-1, co-activator-associated arginine methyltransferase 1; ChIP, chromatin immunoprecipitation; ChIP-qPCR, ChIP quantitative PCR; DMSO, dimethyl sulfoxide; EMSA, electrophoretic mobility shift assay; FXR, Farnesoid X receptor; FXR-KO, FXR knockout; FBS, fetal bovine serum; GSP, gene specific primer; GAPDH, glyceraldehyde 3-phosphate dehydrogenase; GRIP-1, glucocorticoid receptor interacting protein 1; HCC, hepatocellular carcinoma; IACUC, Institutional Animal Care and Use Committee; NCoR, nuclear corepressor; OCA, obeticholic acid; PGC-1α, peroxisome proliferator-activated receptor-gamma coactivator-1alpha; RT-PCR, reverse transcription PCR; RIGSC, Rhode Island Genomic and Sequencing Center; SHP, small heterodimer partner; SRC-1, steroid receptor coactivator 1; TSS, transcription starting site; USP2, Ubiquitin specific peptidase 2; USP2a, USP2 isoform a; USP2b, USP2 isoform b; Wt, wild type.

Address correspondence to: Ruitang Deng, Department of Biomedical and Pharmaceutical Sciences, College of Pharmacy, University of Rhode Island, Kingston, RI 02881, USA. Tel: 401-874-4950; Fax: 401-874-5787; E-mail: dengr@uri.edu

References

[1] Centers for Disease Control and Prevention (CDC). Liver cancer 2022. https://www.cdc.gov/cancer/liver/index.htm.

[2] Surveillance, Epidemiology, and End Results (SEER). Cancer of the Liver and Intrahepatic Bile Duct - Cancer Stat Facts 2022. https://seer.cancer.gov/statfacts/html/livibd.html.

[3] Pinter M, Trauner M, Peck-Radosavljevic M and Sieghart W. Cancer and liver cirrhosis: implications on prognosis and management. ESMO Open 2016; 1: e000042.

[4] Chiang JYL and Ferrell JM. Discovery of farnesoid X receptor and its role in bile acid metabolism. Mol Cell Endocrinol 2022; 548: 111618.
[5] Wang YD, Chen WD, Moore DD and Huang W. FXR: a metabolic regulator and cell protector. Cell Res 2008; 18: 1087-1095.
[6] Yang F, Huang X, Yi T, Yen Y, Moore DD and Huang W. Spontaneous development of liver tumors in the absence of the bile acid receptor farnesoid X receptor. Cancer Res 2007; 67: 863-867.
[7] Zhang L, Wang YD, Chen WD, Wang X, Lou G, Liu N, Lin M, Forman BM and Huang W. Promotion of liver regeneration/repair by farnesoid X receptor in both liver and intestine in mice. Hepatology 2012; 56: 2336-2343.
[8] Chen WD, Wang YD, Meng Z, Zhang L and Huang W. Nuclear bile acid receptor FXR in the hepatic regeneration. Biochim Biophys Acta 2011; 1812: 888-892.
[9] Chen Y, Song X, Valanejad L, Vasilenko A, More V, Qiu X, Chen W, Lai Y, Slitt A, Stoner M, Yan B and Deng R. Bile salt export pump is dysregulated with altered farnesoid X receptor isoform expression in patients with hepatocellular carcinoma. Hepatology 2013; 57: 1530-1541.
[10] Kim I, Morimura K, Shah Y, Yang Q, Ward JM and Gonzalez FJ. Spontaneous hepatocarcinogenesis in farnesoid X receptor-null mice. Carcinogenesis 2007; 28: 940-946.
[11] Komander D and Rape M. The ubiquitin code. Annu Rev Biochem 2012; 81: 203-229.
[12] Jang HH. Regulation of protein degradation by proteasomes in cancer. J Cancer Prev 2018; 23: 153-161.
[13] Mennerich D, Kubaichuk K and Kietzmann T. DUBs, Hypoxia, and cancer. Trends Cancer 2019; 5: 632-653.
[14] Hanpude P, Bhattacharya S, Dey AK and Maiti TK. Deubiquitinating enzymes in cellular signaling and disease regulation. IUBMB Life 2015; 67: 544-555.
[15] Tao BB, He H, Shi XH, Wang CL, Li WQ, Li B, Dong Y, Hu GH, Hou LJ, Luo C, Chen JX, Chen HR, Yu YH, Sun QF and Lu YC. Up-regulation of USP2a and FASN in gliomas correlates strongly with glioma grade. J Clin Neurosci 2013; 20: 717-720.
[16] Graner E, Tang D, Rossi S, Baron A, Migita T, Weinstein LJ, Lechpammer M, Huesken D, Zimmermann J, Signoretti S and Loda M. The isopeptidase USP2a regulates the stability of fatty acid synthase in prostate cancer. Cancer Cell 2004; 5: 253-261.
[17] Wang CL, Wang JY, Liu ZY, Ma XM, Wang XW, Jin H, Zhang XP, Fu D, Hou LJ and Lu YC. Ubiquitin-specific protease 2a stabilizes MDM4 and facilitates the p53-mediated intrinsic apoptotic pathway in glioblastoma. Carcinogenesis 2014; 35: 1500-1509.
[18] Mahul-Mellier AL, Datler C, Pazarentzos E, Lin B, Chaisaklert W, Abuali G and Grimm S. Deubiquitinating proteases USP2a and USP2c cause apoptosis by stabilising RIP1. Biochim Biophys Acta 2012; 1823: 1353-1365.
[19] Kitamura H and Hashimoto M. USP2-related cellular signaling and consequent pathophysiological outcomes. Int J Mol Sci 2021; 22:1209.
[20] Baek SH, Choi KS, Yoo YJ, Cho JM, Baker RT, Tanaka K and Chung CH. Molecular cloning of a novel ubiquitin-specific protease, UBP41, with isopeptidase activity in chick skeletal muscle. J Biol Chem 1997; 272: 25560-25565.
[21] Gousseva N and Baker RT. Gene structure, alternate splicing, tissue distribution, cellular localization, and developmental expression pattern of mouse deubiquitinating enzyme isoforms Usp2-45 and Usp2-69. Gene Expr 2003; 11: 163-179.
[22] Zhu HQ and Gao FH. The molecular mechanisms of regulation on usp2's alternative splicing and the significance of its products. Int J Biol Sci 2017; 13: 1489-1496.
[23] Nadolny C, Zhang X, Chen Q, Hashmi SF, Ali W, Hemme C, Ahsan N, Chen Y and Deng R. Dysregulation and activities of ubiquitin specific peptidase 2b in the pathogenesis of hepatocellular carcinoma. Am J Cancer Res 2021; 11: 4746-4767.
[24] Zhang X, Nadolny C, Chen Q, Ali W, Hashmi SF and Deng R. Dysregulation and oncogenic activities of ubiquitin specific peptidase 2a in the pathogenesis of hepatocellular carcinoma. Am J Cancer Res 2023; 13: 2392-2409.
[25] Chen Y, Vasilenko A, Song X, Valanejad L, Verma R, You S, Yan B, Shiffka S, Hargreaves L, Nadolny C and Deng R. Estrogen and estrogen receptor-alpha-mediated transrepression of bile salt export pump. Mol Endocrinol 2015; 29: 613-626.
[26] Song X, Vasilenko A, Chen Y, Valanejad L, Verma R, Yan B and Deng R. Transcriptional dynamics of bile salt export pump during pregnancy: mechanisms and implications in intrahepatic cholestasis of pregnancy. Hepatology 2014; 60: 1993-2007.
[27] You S, Cui AM, Hashmi SF, Zhang X, Nadolny C, Chen Y, Chen Q, Bush X, Hurd Z, Ali W, Qin G and Deng R. Dysregulation of bile acids increases the risk for preterm birth in pregnant women. Nat Commun 2020; 11: 2111.
[28] Pouly D, Chenaux S, Martin V, Babis M, Koch R, Nagoshi E, Katanaev VL, Gachon F and Staub O. USP2-45 is a circadian clock output effector regulating calcium absorption at the

post-translational level. PLoS One 2016; 11: e0145155.
[29] Umarov RK and Solovyev VV. Recognition of prokaryotic and eukaryotic promoters using convolutional deep learning neural networks. PLoS One 2017; 12: e0171410.
[30] Hoeke MO, Heegsma J, Hoekstra M, Moshage H and Faber KN. Human FXR regulates SHP expression through direct binding to an LRH-1 binding site, independent of an IR-1 and LRH-1. PLoS One 2014; 9: e88011.
[31] Bramlett KS, Yao S and Burris TP. Correlation of farnesoid X receptor coactivator recruitment and cholesterol 7alpha-hydroxylase gene repression by bile acids. Mol Genet Metab 2000; 71: 609-615.
[32] Mi LZ, Devarakonda S, Harp JM, Han Q, Pellicciari R, Willson TM, Khorasanizadeh S and Rastinejad F. Structural basis for bile acid binding and activation of the nuclear receptor FXR. Mol Cell 2003; 11: 1093-1100.
[33] Ananthanarayanan M, Li S, Balasubramaniyan N, Suchy FJ and Walsh MJ. Ligand-dependent activation of the farnesoid X-receptor directs arginine methylation of histone H3 by CARM1. J Biol Chem 2004; 279: 54348-54357.
[34] Rosenfeld MG, Lunyak VV and Glass CK. Sensors and signals: a coactivator/corepressor/epigenetic code for integrating signal-dependent programs of transcriptional response. Genes Dev 2006; 20: 1405-1428.
[35] Liu N, Meng Z, Lou G, Zhou W, Wang X, Zhang Y, Zhang L, Liu X, Yen Y, Lai L, Forman BM, Xu Z, Xu R and Huang W. Hepatocarcinogenesis in FXR-/- mice mimics human HCC progression that operates through HNF1alpha regulation of FXR expression. Mol Endocrinol 2012; 26: 775-785.
[36] Martinez-Becerra P, Vaquero J, Romero MR, Lozano E, Anadon C, Macias RI, Serrano MA, Grane-Boladeras N, Munoz-Bellvis L, Alvarez L, Sangro B, Pastor-Anglada M and Marin JJ. No correlation between the expression of FXR and genes involved in multidrug resistance phenotype of primary liver tumors. Mol Pharm 2012; 9: 1693-1704.
[37] Su H, Ma C, Liu J, Li N, Gao M, Huang A, Wang X, Huang W and Huang X. Downregulation of nuclear receptor FXR is associated with multiple malignant clinicopathological characteristics in human hepatocellular carcinoma. Am J Physiol Gastrointest Liver Physiol 2012; 303: G1245-G1253.
[38] Suda T, Yokoo T, Kanefuji T, Kamimura K, Zhang G and Liu D. Hydrodynamic delivery: characteristics, applications, and technological advances. Pharmaceutics 2023; 15: 1111.
[39] Liu F, Song Y and Liu D. Hydrodynamics-based transfection in animals by systemic administration of plasmid DNA. Gene Ther 1999; 6: 1258-1266.
[40] Ho C, Wang C, Mattu S, Destefanis G, Ladu S, Delogu S, Armbruster J, Fan L, Lee SA, Jiang L, Dombrowski F, Evert M, Chen X and Calvisi DF. AKT (v-akt murine thymoma viral oncogene homolog 1) and N-Ras (neuroblastoma ras viral oncogene homolog) coactivation in the mouse liver promotes rapid carcinogenesis by way of mTOR (mammalian target of rapamycin complex 1), FOXM1 (forkhead box M1)/SKP2, and c-Myc pathways. Hepatology 2012; 55: 833-845.
[41] Engelholm LH, Riaz A, Serra D, Dagnaes-Hansen F, Johansen JV, Santoni-Rugiu E, Hansen SH, Niola F and Frodin M. CRISPR/Cas9 engineering of adult mouse liver demonstrates that the Dnajb1-prkaca gene fusion is sufficient to induce tumors resembling fibrolamellar hepatocellular carcinoma. Gastroenterology 2017; 153: 1662-1673, e1610.
[42] Moon H, Ju HL, Chung SI, Cho KJ, Eun JW, Nam SW, Han KH, Calvisi DF and Ro SW. Transforming growth factor-beta promotes liver tumorigenesis in mice via up-regulation of snail. Gastroenterology 2017; 153: 1378-1391, e1376.
[43] Gao M and Liu D. CRISPR/Cas9-based Pten knock-out and sleeping beauty transposon-mediated Nras knock-in induces hepatocellular carcinoma and hepatic lipid accumulation in mice. Cancer Biol Ther 2017; 18: 505-512.
[44] Herweijer H, Zhang G, Subbotin VM, Budker V, Williams P and Wolff JA. Time course of gene expression after plasmid DNA gene transfer to the liver. J Gene Med 2001; 3: 280-291.
[45] Wooddell CI, Reppen T, Wolff JA and Herweijer H. Sustained liver-specific transgene expression from the albumin promoter in mice following hydrodynamic plasmid DNA delivery. J Gene Med 2008; 10: 551-563.
[46] Wang X, Fu X, Van Ness C, Meng Z, Ma X and Huang W. Bile acid receptors and liver cancer. Curr Pathobiol Rep 2013; 1: 29-35.
[47] Sun L, Cai J and Gonzalez FJ. The role of farnesoid X receptor in metabolic diseases, and gastrointestinal and liver cancer. Nat Rev Gastroenterol Hepatol 2021; 18: 335-347.
[48] Luo W, Guo S, Zhou Y, Zhu J, Zhao J, Wang M, Sang L, Wang B and Chang B. Hepatocellular carcinoma: Novel understandings and therapeutic strategies based on bile acids (Review). Int J Oncol 2022; 61: 117.